



HAL
open science

Gasification of woodchip particles: Experimental and numerical study of char–H₂O, char–CO₂, and char–O₂ reactions

L. van de Steene, J.P. Tagutchou, Francisco Javier Escudero Sanz, Sylvain Salvador

► To cite this version:

L. van de Steene, J.P. Tagutchou, Francisco Javier Escudero Sanz, Sylvain Salvador. Gasification of woodchip particles: Experimental and numerical study of char–H₂O, char–CO₂, and char–O₂ reactions. *Chemical Engineering Science*, 2011, 66 (20), pp.4499-4509. 10.1016/j.ces.2011.05.045 . hal-01801197

HAL Id: hal-01801197

<https://imt-mines-albi.hal.science/hal-01801197>

Submitted on 1 Jun 2018

HAL is a multi-disciplinary open access archive for the deposit and dissemination of scientific research documents, whether they are published or not. The documents may come from teaching and research institutions in France or abroad, or from public or private research centers.

L'archive ouverte pluridisciplinaire **HAL**, est destinée au dépôt et à la diffusion de documents scientifiques de niveau recherche, publiés ou non, émanant des établissements d'enseignement et de recherche français ou étrangers, des laboratoires publics ou privés.

Gasification of woodchip particles: Experimental and numerical study of char–H₂O, char–CO₂, and char–O₂ reactions

L. Van de steene^{a,*}, J.P. Tagutchou^a, F.J. Escudero Sanz^b, S. Salvador^b

^a CIRAD-PERSYST, UPR 42 Biomass Energy, TA B42/16, 73 rue JF Breton, 34398 Montpellier Cedex 5, France

^b RAPSODEE, Ecole des Mines d'Albi-Carmaux, Campus Jarlard, 81013 ALBI Cedex 09, France

ABSTRACT

In wood gasification, oxidation of char particles by H₂O, CO₂ or O₂ plays a major role in the performance and efficiency of air gasifiers. These reactions are generally analyzed under carefully design and controlled laboratory conditions, using either micro-samples to focus on the reaction kinetics or large spherical particles, but rarely using the real shape encountered in industrial processes. The objective of this work was to conduct a complete parametric study on char gasification kinetics at particle scale in operating conditions like those of industrial applications. Experimental results from a macro-Thermo Gravimetric reactor are compared to those from a char particle model, which analyzes reactivity versus conversion through the surface function $F(X)$.

We first show that particle thickness is a representative dimension of a char particle with respect to its apparent kinetics. Second, considering the three reactions independently, we compared the influence of temperature (800–1050 °C) and reacting gas partial pressure (0.03–0.4 atm) and determined the intrinsic kinetic parameters and surface function $F(X)$. Simulations provided profiles of temperature and gas concentrations within the particle, mainly revealing internal mass diffusion limitation. The experimental data base proposed and the model results improve our understanding of the gasification reaction and support the elaboration of process models.

Keywords:

Energy
Gasification
Kinetics
Particle
Fuel
Wood

1. Introduction

Gasification has recently been receiving increasing attention thanks to the success of the first plants for the production of electricity from biomass (Knoef, 2005). The increasing interest in such processes is due to the high potential of biomass resources. Most of the reliable demonstration plants are fueled with wood chips, which is the simplest biomass in terms of availability and standardization. Even so, the economic viability of fixed bed wood gasifiers remains questionable because of high investment and maintenance costs, which are the consequence of the bad quality of the fuel gas and poor energy efficiency due to high residual carbon in the ash. A gasification process consists of a sequence of complex chemical reactions, mainly drying and pyrolysis of the wood, homogeneous oxidation of pyrolysis gases, and heterogeneous oxidation of residual carbon. In the more advanced fixed bed technologies, these reactions occur in separate reactors or zones thus allowing better control of each reaction. Achieving complete carbon conversion is mainly controlled by the heterogeneous reactions that occur between the char produced during

the pyrolysis stage, and the reacting gases such as H₂O, CO₂ and O₂. These reacting gases result from the drying, pyrolysis and homogeneous oxidation steps.

Steam attack is known to play a major role in carbon transformation both in terms of conversion rapidity and hydrogen yield. Though to a lesser extent, carbon dioxide also participates in carbon conversion: its reaction kinetics is known to be at a ratio of 2:5 slower depending on the temperature and concentration levels (Van den Aarsen et al., 1985). The contribution of oxygen is important as it is the only significant exothermic reaction in the char gasification zone that ensures the temperature is high enough for acceptable carbon conversion. Regarding kinetics, its influence on the global process is less significant as C–O₂ reaction is known to be much faster than C–CO₂ and C–H₂O reactions at atmospheric pressure (Dutta et al., 1977; Dutta and Wen, 1977; Harris and Smith, 1990) and high pressure (Roberts and Harris, 2000).

Understanding of the relative contribution of each reaction, and quantifying the influence on carbon conversion of temperature, the nature and concentration of the gas, and of particle dimensions is of primary importance in the design and optimization of new gasifiers. These points represent the main contribution of this work.

These reactions are commonly described as heterogeneous surface reactions with the following stages: firstly, adsorption of the reacting gas on the free active carbon sites; secondly, C–Gas

* Corresponding author. Tel.: +33 0 4 67 61 65 22; fax: +33 0 4 67 61 65 15.
E-mail address: steene@cirad.fr (L. Van de steene).

reaction ($\text{Gas}=\text{H}_2\text{O}$, CO_2 or O_2), and finally, desorption of the resulting gases H_2 , CO , and CO_2 . The influence of operating conditions on the gasification kinetics of different wood chars and coals is widely reported in the literature, with both CO_2 and H_2O as the oxidant (Di Blasi, 2009; Klose and Wolki, 2005; Standish and Tanjung, 1988). In particular, char gasification is known to be very sensitive to temperature and to partial pressure of the oxidant.

But many of these investigations were undertaken in kinetic-controlled regimes with simple configurations in which heat and mass transfer are not significant, i.e., at the microscopic scale using a Thermo Gravimetric Analysis reactor. However, in industrial processes, where particle size is often larger than 1 mm, the gasification reaction is also controlled by heat and mass transfer. Consequently, the extrapolation of results in kinetic-controlled regimes to larger particle is not easy, as modeling of intra-particle transfers remains complex. Indeed, heat and mass transfer both within the particle and outside are highly dependent on the structure of the char, i.e. reactive surface area, porosity, and tortuosity (Sorensen et al., 1996; Sharma et al., 2002; Groeneveld and van Swaaij, 1980; Cetin et al., 2005).

For this reason, some authors investigated gasification at a macro-particle scale to characterise such internal transfer mechanisms (Standish and Tanjung 1988; Kumar and Gupta 1994; Dasappa et al., 1994). The influence of the size of the particles on gasification was carefully examined by some authors (Standish and Tanjung 1988; Ye et al., 1998; Kovacik et al., 1991) who showed a decrease in apparent kinetics with an increase in particle size. This confirms the presence of a transfer limited regime above a critical particle size, which depends on the nature of the fuel and on intrinsic reaction kinetics. In a previous work, Mermoud et al. (2006) conducted a complete parametric study of the steam gasification of beech charcoal spheres of different diameters (10–30 mm). Comparisons between experimental data and predictions of a 1-D model were both qualitatively and quantitatively satisfactory and enabled determination of the intrinsic constants of their LH-type kinetic model.

Up to now, little attention has been paid to the characterization of industrial-shaped particles during their thermochemical conversion in the operating conditions of a fixed-bed gasifier. Indeed, in industrial processes, particles are not spherical and size measured by standard sieving is not a characteristic dimension of the apparent kinetics of gasification. Heat and mass transfer differ significantly depending on the shape of the particle. This is shown for example by the divergence in heat and mass transfer coefficient depending on whether the particle is spherical, cylindrical or flake. Groeneveld and van Swaaij (1980) compared flake and spherical particles during gasification and concluded that at constant particle volume, spherical particles were less reactive. A few other authors conducted experiments to determine the influence of particle shape on gasification (Henriksen et al., 2006; Moilanen et al., 1993; De Diego et al., 2002). Henriksen et al. (2006) investigated the behavior of parallelepiped pieces of wood and revealed the influence of the dimensions on the rate of conversion. Experimentally, he showed that char reactivity was considerably higher when the particle was positioned so that the fibers were in the direction of the reactant gas flow. This was confirmed by Moilanen et al. (1993) with larger biomass particles. This phenomenon is particularly true in the case of wood due to its strong anisotropy, and the same goes for char produced from wood.

The purpose of this study was to investigate the gasification of char particles using a fundamental approach. The present work enabled us to estimate the gasification kinetics of charcoal particles from wood chips in three atmospheres (steam, carbon dioxide, and oxygen), in concentrations and temperatures that are applicable to industrial air gasifiers: Temperature: 800–1000 °C;

$[\text{H}_2\text{O}]$: 0.1–0.3 atm, $[\text{CO}_2]$: 0.1–0.3 atm, $[\text{O}_2]$: 0.03–0.12 atm. The role of particle dimensions is another important point in this paper. This research may provide useful information and data for the modeling and design of gasification processes.

In the following section (Section 2), we present an experimental program based on macro-thermogravimetry experiments. Then we discuss the results of the complete parametric study with particular attention to the identification of the critical dimension. In Section 3, we describe the modifications that were made to the numerical model from Mermoud et al. (2006) and compare and discuss the experimental and numerical results. In Section 4, we describe how exploitation of the model provides the concentration and temperature fields within the particle, which enable evaluation of heat and mass transfer limitations in typical operating conditions.

2. Experimental study

2.1. Description of the experiments

The apparatus used was a “macro-TG” reactor (Fig. 1), previously described in detail in Mermoud et al. (2006). Roughly, it consists of a 2-m long, 80-mm i.d. quartz reactor electrically heated to a maximum temperature of 1050 °C. Three zones are independently controlled to ensure good temperature homogeneity throughout the reactor. Before entering the reactor, the reactant gas (N_2 with H_2O , CO_2 or O_2) crosses a preheater, which enables the gas to reach

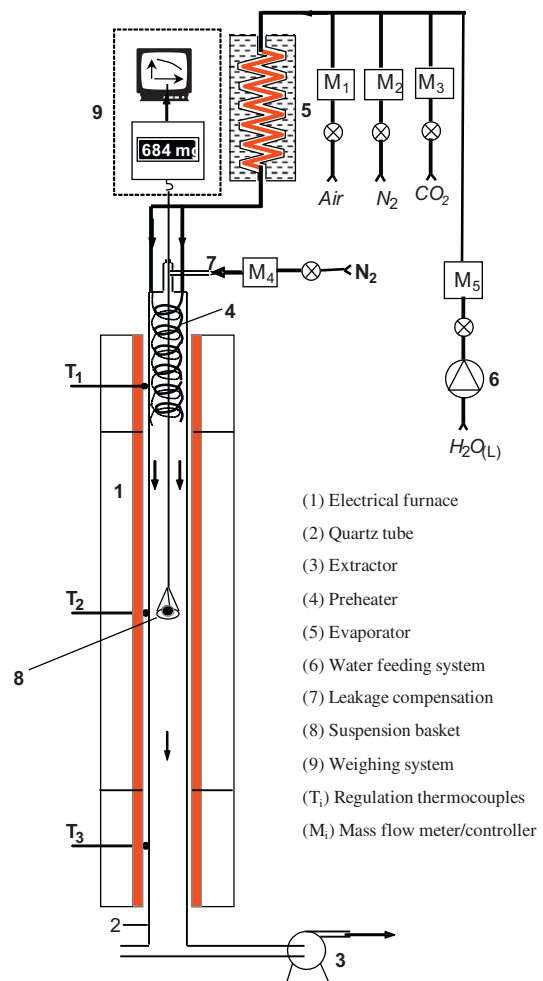


Fig. 1. Experimental macro-TG.

the temperature of the reactor (800–1000 °C). When steam is used for experiments, the H₂O/N₂ mix first passes through an electrically heated evaporator at 200 °C to vaporize the water. The flow rates of N₂, H₂O, CO₂, O₂ are controlled by mass flow meters/controllers. In our experiment, a few particles were placed in a grid basket, which was suspended inside the reactor and continuously weighed with an accuracy of ±1 mg. Atmosphere flow is laminar, the average velocity of the reactant gas was maintained at 0.14 m/s; in a previous study we showed that this velocity did not influence gasification in our operating conditions Mermoud et al. (2006).

The operating conditions in terms of temperature, steam partial pressure, and gas velocity around the particle were well controlled, which is essential for an accurate parametric study. Experiments were conducted at atmospheric pressure in the following operating conditions, covering those encountered in the char gasification zone of air gasifiers:

- temperature: 800, 900, 1000, and 1050 °C;
- partial pressure of reacting gas:
 - 0.1, 0.2 or 0.4 atm for H₂O;
 - 0.1, 0.2 or 0.4 atm for CO₂; and
 - 0.03, 0.06, and 0.12 atm for O₂.

For each experiment, the reactor was first heated to the operating temperature under N₂ atmosphere. The basket was then lifted from the bottom of the reactor, and hung on the load cell. The constant mass achieved under N₂ ensured that the gas adsorbed at the surface of the charcoal (moisture, hydrocarbons remaining after pyrolysis) was released before gasification with H₂O, CO₂ or O₂. The reactant gas flow was then established, producing the desired atmosphere and marking the initial time. When reacting, the mass of the sample progressively decreased

until a constant mass – that of ash – was reached to conclude the test. The mass of the sample was continuously recorded during the test enabling us to calculate the conversion over time.

2.2. Wood feedstock and char preparation

Wood chips made from French maritime pine, like those used in industrial wood boilers, were used. Results of proximate and ultimate analyses of the initial wood, obtained in compliance with standards are listed in Table 1.

Char particles were prepared from wood chips by successive pyrolysis to produce charcoal, and selection of the appropriate size. We used a screw pyrolysis reactor externally heated by electrical heating elements as described elsewhere (Fassinou et al., 2009). The objective of char production was to obtain a char with low volatile matter content in order to focus on heterogeneous char gasification reaction. The operating conditions were as follows: 750 °C temperature, 1 h residence time, and 15 kg/h wood chip mass flow rate. The heating rate, which is known to have a significant influence on charcoal gasification (Mermoud et al., 2006), was about 50 K/min (Fassinou et al., 2009).

Results of proximate and ultimate analyses of the prepared charcoal are listed in Table 1. The residual volatile content was lower than 5%.

Fig. 2 shows photographs of wood chips before (a) and after (b) pyrolysis. Despite the standardization of wood chips, the size and shape of the particles were heterogeneous. Particle size distribution of the charcoal from pyrolysis of wood chips is shown in Fig. 3: 80% of the weight of the sample particles was in the granulometry range of 2–12 mm. The mean particle size according to the Rosin–Rammler model was calculated as 5.6 mm.

2.3. Experimental results

The conversion ratio during gasification by steam, carbon dioxide, or oxygen was calculated according to Eq. (1):

$$X = \frac{m_{init} - m}{m_{init} - m_{ash}} \quad (1)$$

where m , m_{init} , m_{ash} are respectively the mass at time t , the initial mass and the mass of ashes.

All the experiments were carried out several times to check repeatability. A deviation of about 10% in the results was observed. This repeatability is acceptable considering the heterogeneity of the wood and the large size of the particles. Some dispersion remained, showing that repeating all the experiments was necessary. All the data presented are an average of 3 repeatability experiments.

Table 1
Proximate and ultimate analyses of wood chips and charcoal from maritime pine.

Material	Wood chips	Char
Proximate analysis (wt%)		
Moisture (as received)	12	1.8
Ash (dry basis)	0.2	1.4
Volatile matter (dry basis)	82.6	4.9
Fixed carbon (dry basis by difference)	17.2	93.7
Ultimate analysis (wt% on dry)		
C	47.8	89.8
H	6.1	2.2
O	45.5	6.1
N	< 0.3	0.1
S	< 0.1	0.001

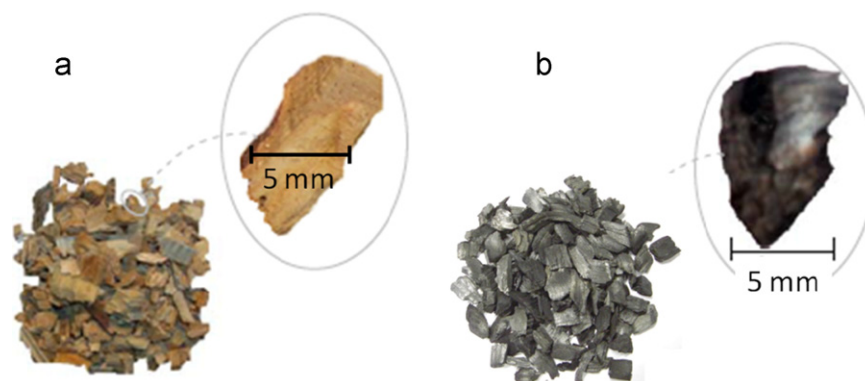


Fig. 2. Photograph of a sample of maritime pine wood chip particles before (a) and after (b) pyrolysis.

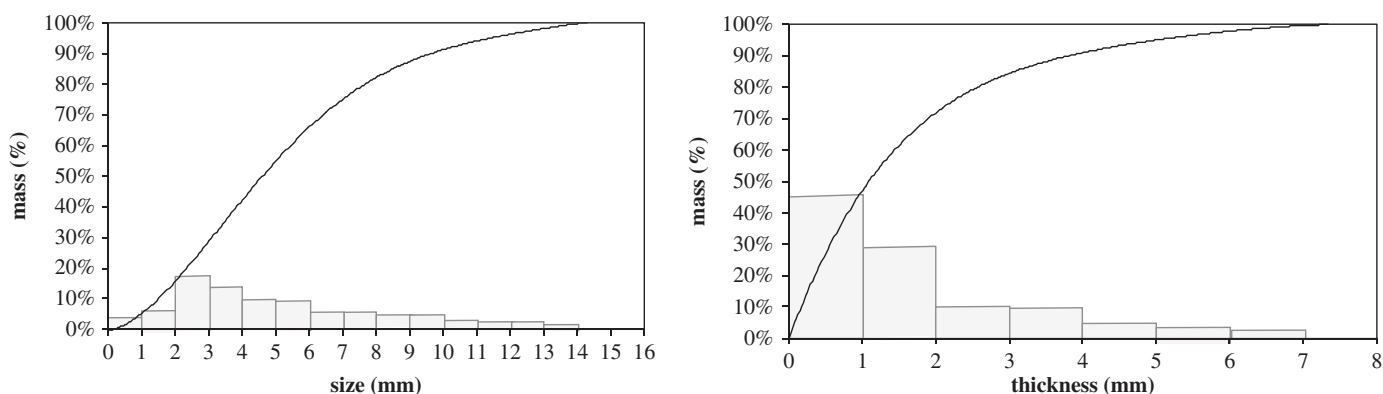


Fig. 3. Particle size and thickness mass distribution.

Table 2

Operating conditions of the experiments.

Reacting gas	
H ₂ O (atm)	0.1, 0.2, 0.4
CO ₂ (atm)	0.1, 0.2, 0.4
O ₂ (atm)	0.03, 0.06, 0.12
T (°C)	800, 900, 1000, 1050

Experiments were performed with several particles (four–six) in the grid basket to increase the signal/noise ratio of the load cell by increasing the total mass of the sample. Above all, using several particles enabled us to average weight loss for the different particles and freed us from the need to consider the heterogeneous composition of the particles. To avoid thermal and chemical interactions between the particles, we arranged them on a horizontal plane so that there was no contact between them. Operating conditions of the experiments are listed in Table 2.

2.3.1. Role of dimensions

The role of particle size, determined by standard sieving, and of thickness (the smallest dimension) was determined by the following set of experiments:

- First, we selected particles with the same thickness (5.5 mm) but of different size (10.5, 13, 15 mm).
- Second, we chose particles of the same size (10.5 mm) but with different thicknesses (1.5, 2.5, 4.5, 5.5, 6.5 mm).

Experiments were conducted in a 0.2 atm H₂O in N₂ atmosphere at 900 °C.

The conversion ratio versus gasification time is plotted in Fig. 4. In the size range considered, gasification was not influenced by the largest dimension of the particle, since reducing the size of particles did not significantly change the conversion ratio (Fig. 4a). Conversely, when we varied only the thickness of the particle, the conversion ratio was sensitive to the dimension (Fig. 4b). A particle 1.5 mm thick was converted in 1500 s whereas a particle 6.5 mm thick needed 2400 s, i.e. was 1.6 times slower. We can therefore conclude that gasification of wood chip particles is limited by heat and/or mass external and/or internal transfer. We propose to consider the thickness of the particle as the characteristic dimension, and it will be used in the sequel to this paper. Moreover, there was no significant difference in conversion ratio for particle thickness of 2.5 mm or 1.5 mm. This result suggests that below 2.5 mm, particle thickness did not influence significantly the gasification process.

2.3.2. Role of temperature

The role of the temperature was evaluated thanks to experiments with temperatures varying between 800 and 1050 °C, successively in 0.2 atm of H₂O in N₂ and in 0.2 atm of CO₂ in N₂.

Gasification by steam (Fig. 5a) or carbon dioxide (Fig. 5b) was sensitive to temperature. Indeed, in H₂O atmosphere, the complete conversion was reached after 5400, 1860, and 600 s at temperatures of 800, 900, and 1000 °C respectively. That is to say a 200 °C increase in gasification temperature resulted in nine times higher reactivity.

The same trend was observed for gasification with carbon dioxide (Fig. 5b). Experiments at 800 °C were not performed, as at this temperature the conversion rate is too low to play a significant role in char gasification kinetics. In this case, the experiment was performed at 1050 °C to evaluate the sensitivity of the reaction to temperature.

One should mention that it was not possible here to dissociate the effects of temperature and thermal annealing on the conversion. Indeed, the chars studied at the 3 temperatures did not follow the same thermal history as each of them are heated in N₂ atmosphere and maintained few minutes to a different reaction temperature prior to gasification.

2.3.3. Role of partial pressure of reacting gas

At the reference temperature of 900 °C, we varied the concentration of the reactant gas in each atmosphere (Fig. 6).

In steam atmosphere, gasification was completed at 2460, 1860, and 900 s with 0.1, 0.2 and 0.4 atm H₂O (in N₂), respectively (Fig. 6a). Steam gasification was thus about 3 times faster with 0.4 atm H₂O than with 0.1 atm H₂O.

In carbon dioxide atmosphere, gasification was completed after 6900 s with 0.1 atm CO₂ while it was completed only after 3000 s with 0.4 atm CO₂ (Fig. 6b). CO₂ gasification was thus 2.3 times faster with 0.4 atm CO₂ than with 0.1 atm CO₂.

In oxygen atmosphere, char oxidation was determined at 0.03, 0.06, and 0.12 atm O₂ (in N₂). Experiments with high O₂ partial pressure were not justified, because the oxygen concentration is low in the char gasification zone of gasifiers. The reaction was completed after 660, 1320, and 2400 s with 0.12, 0.06, and 0.03 atm oxygen, respectively (Fig. 6c).

Fig. 7 shows the conversion progresses in the three atmospheres (H₂O, CO₂, and O₂). Gasification of our wood char at 900 °C was about 3 times faster in 0.2 atm H₂O than in 0.2 atm CO₂. This result is in agreement with results reported in the literature by several authors, showing that gasification with carbon dioxide is two to five times slower than with steam (Van den Aarsen et al., 1985; Harris and Smith, 1990; Rensfelt et al., 1978). This gap is probably due to the difference in intrinsic chemical kinetics of C–H₂O reactions and C–CO₂.

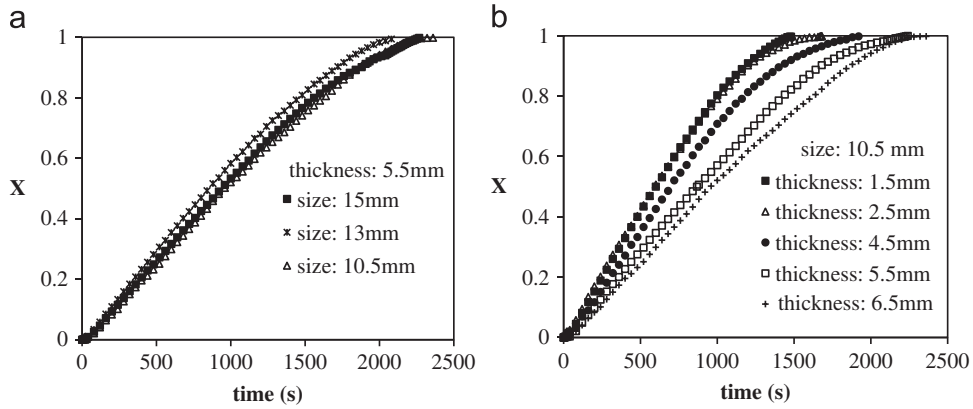


Fig. 4. Influence of particle size (a) and particle thickness (b) on the steam gasification conversion rate (bulk gas temperature: 900 °C, 0.2 atm H₂O (in N₂)).

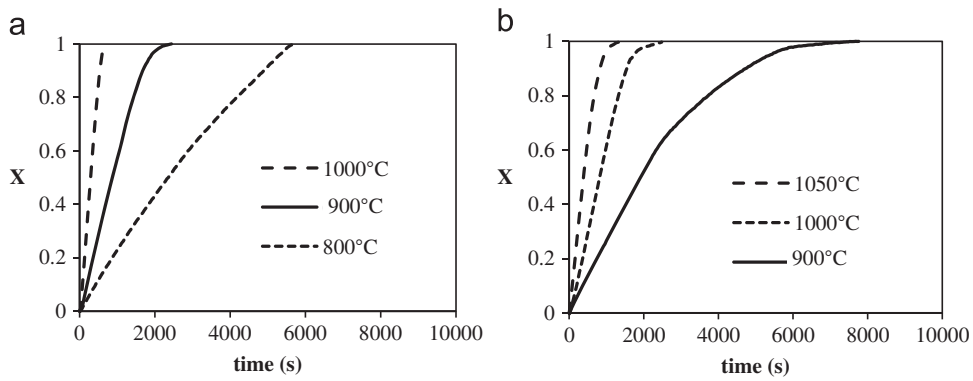


Fig. 5. Influence of bulk temperature in H₂O atmosphere (a) and CO₂ atmosphere (b). (partial pressure of reactant gas: 0.2 atm, particle size: 10.5 mm, and particle thickness: 5.5 mm).

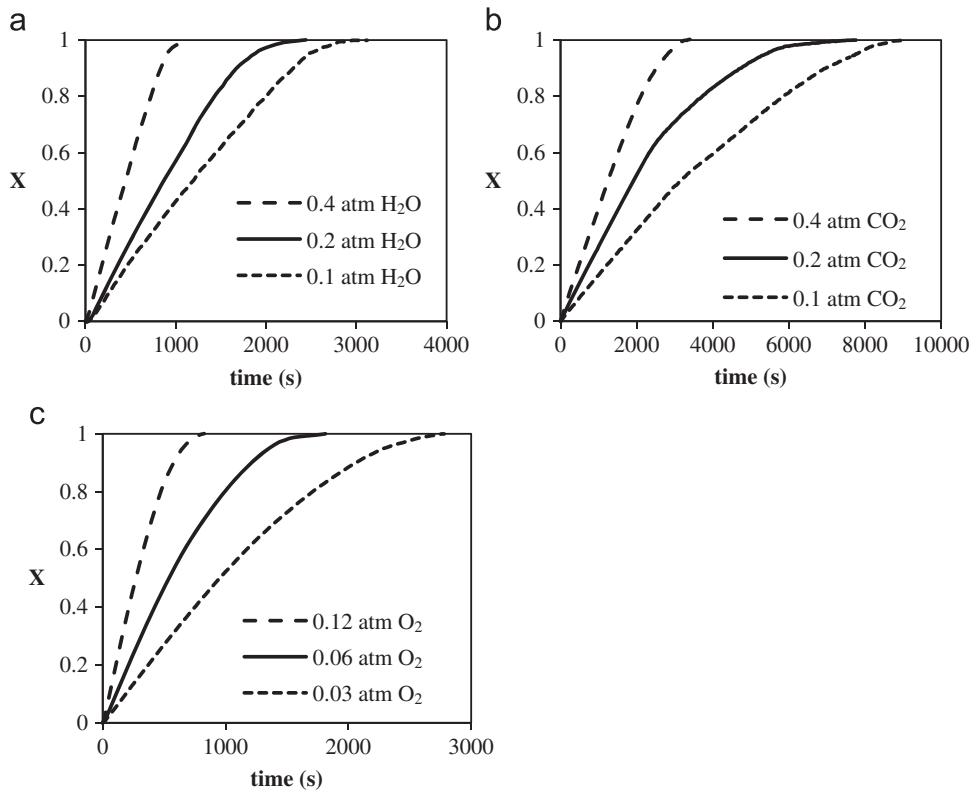


Fig. 6. Influence of partial pressure of reactant gas: H₂O (a), CO₂ (b), O₂ (c). (temperature of bulk gas: 900 °C, particle thickness: 5.5 mm, and particle size 10.5 mm).

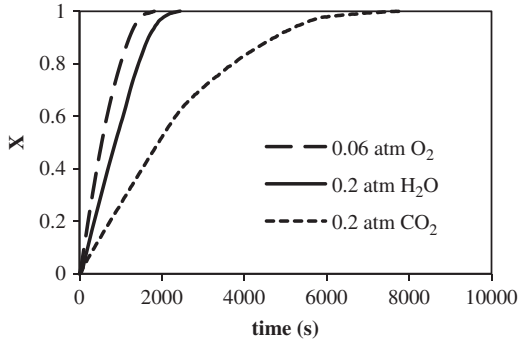


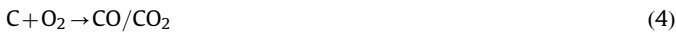
Fig. 7. Comparison of the conversion ratios in the three atmospheres (temperature of bulk gas: 900 °C, particle thickness: 5.5 mm, and particle size: 10.5 mm).

In a previous study, for steam gasification, we showed that the conversion derivative (dX/dt) was quasi-constant along nearly 90% of the conversion process. This is a specificity of biomass char compared to coal char (Mermoud et al., 2006). This result is confirmed here in Fig. 7.

In experiments in 0.2 atm CO_2 , the shape of the curve differed from the others with a clear break in the slope at about 60% of conversion. The same behavior was observed in a 0.1 atm CO_2 (Fig. 6b) where the break appeared earlier (at 50% conversion). This phenomenon does not appear at higher temperatures or under higher CO_2 partial pressure. At this stage, we have no explanation for this phenomenon.

3. Numerical study

The model developed enables prediction of the gasification of a char particle in an H_2O , CO_2 or O_2 atmosphere according to the following reactions:



The model, originally developed to predict the steam gasification of a spherical particle of wood char, is described in detail elsewhere (Mermoud et al., 2006). Briefly, the charcoal particle can be seen as a porous medium including a fluid and a solid region consisting mainly of carbon. The main simplifying assumptions are listed below:

- macroscopic properties (pressure, concentration, temperature) are assumed to be uniform at the charcoal surface and the particle is considered to remain spherical throughout gasification,
- tar formation is not taken into account,
- diffusive transport is assumed to be governed by the Fick law, and
- Dufour and Soret effects are not considered.

Under these assumptions, the overall mass, species, and energy conservation equations have been simplified into the spherically symmetric, one-dimensional form.

To conform with the objective of the present work, the model was improved in order to consider:

- (i) Boudouard (Eq. (3)) and combustion (Eq. (4)) reactions.
- (ii) The non-sphericity of the particle.

- (iii) The change in the morphological structure of the char by the introduction of a surface function $F(X)$ (which is discussed later on).

Regarding (ii), the non-sphericity of the particle was considered by introducing new external coefficients for heat and mass transfer. Hobbs et al. (1993) explained that the solid/gas heat transfer coefficient estimated from non-reacting system data is different from the one in reacting gasifiers, as a consequence of unsteady heat transfer. Therefore, the experimental correlation was multiplied by an empirical factor (ξ) (with values in the range of 0.02–1 (Hobbs et al., 1993; Cho and Joseph, 1981; Di Blasi, 2000)). Moreover, other aspects such as roughness of the surface or irregular shape of the particle can influence external heat/mass transfer. Consequently, we introduced a correction factor (ξ) in our model to account for the complexity of the reacting media regarding the determination of these coefficients.

The Nusselt number was calculated for a flat plate as follows:

$$Nu = \xi(0.644Re^{0.5}Pr^{1/3}) \quad (5)$$

where Pr and Re are respectively the Prandtl and the Reynolds number

Then, using Chilton–Colburn analogy (Bhatia and Vartak, 1996) between heat and mass transfer, the Sherwood number was expressed as

$$Sh = \xi(0.644Re^{0.5}Sc^{1/3}) \quad (6)$$

where Sc is the Schmidt number.

The reactivity $R(t)$ can be expressed as a function of the conversion process, X

$$R(t) = -\frac{1}{m} \frac{dm}{dt} = \frac{1}{1-X} \frac{dX}{dt} \quad (7)$$

Whatever the reaction concerned (Eqs. (2)–(4)), char reactivity $R(t)$ depends on temperature, gas partial pressure (n -order dependence) and concentration of active sites

$$R(t) = k_i^{int} P_i^n C_i(t) \quad (8)$$

where, k_i^{int} is the intrinsic reactivity of the reactant gas i , P_i , the partial pressure, and $C_i(t)$, the concentration of active sites.

The temperature dependence of the intrinsic reactivity is given by

$$k_i = A_i e^{-E_i/RT} \quad [\text{mol/mol}] \quad (9)$$

The proportion of CO and CO_2 produced by the combustion reaction (Eq.(4)) was calculated from (Biggs and Agarwal, 1997)

$$\frac{\text{CO}}{\text{CO}_2} = 70e^{-3070/T} \quad [\text{mol/mol}] \quad (10)$$

The concentration of active sites $C_i(t)$ is known to vary with char conversion due to many physical and chemical phenomena (Klose and Wolki, 2005; Mermoud et al., 2006). Moreover, there is a serious difficulty concerning the identification, measurement, identification, and characterization of $C_i(t)$. In fact, many experimental factors affect the determination of $C_i(t)$: temperature, pressure of the reactant and inert gas agent, adsorption stoichiometry, and difficulties involved in perfectly conducting chemisorption without a risk of reaction. As a result, the many attempts to correlate $C_i(t)$ with carbon gasification reactivity have mostly led to scattered correlations.

Two types of models can be used to correlate morphological changes in char reactivity during gasification: models which consider the major phenomena encountered during the conversion, or empirical models determined from experimental data. The former models lead to the consideration of various types of models of morphological structure of char. Many mathematical models are found in the literature, which express the dependence

of the reactivity with the conversion X : shrinking core model, random pore model (Bhatia and Perlmutter, 1980), discrete random pore model (Bhatia and Vartak, 1996), and modified random pore model (Rensfelt et al., 1978). None of these models is capable of accurately describing all the phenomena observed experimentally. Most assume the homogeneity of the particle surface, i.e. the concentration of active sites is considered to remain constant during conversion. This emphasizes the need for an empirical determination of a function that depends on the conversion progress X rather than an a priori decision on a model of structure changes. This function $F(X)$, hereafter called *surface function*, describes the change in the concentration of active sites. It enables all the phenomena involved in the change in reactivity during gasification to be taken into account (Roberts and Harris, 2000). Considering $F(X)$, the reactivity is written

$$R(t) = k^{int} P^n F(X) \quad (11)$$

3.1. Determination of surface functions

From experimental results, $F(X_i)$ can be calculated at any conversion X_i , as follows:

$$F(X_i) = \frac{R(X_i)}{R(X_0)} \quad (12)$$

where $R(X_0)$ is the reactivity at a reference conversion progress. The choice of X_0 is discussed below.

A regression is applied to the $(X_i, F(X_i))$ to determine an analytical function for $F(X)$; polynomial regressions are usually used (Tagutchou, 2008).

The uncertainty in the measured reactivity (Eq. (7)) is often large for low conversion as sensitivity to weight loss is low, and also for the highest conversion, as the mass goes to zero and the reactivity increases considerably. Thus, the normalized reactivity $-R(X)/R(X_0)$ is calculated within a defined interval of X where uncertainties are acceptable. Some authors, including Sorensen (Sorensen et al., 1996), worked on an interval of conversion ranging from 20% to 80%. In the present work, the calculation was made with an X interval ranging from 0.15 to 0.9. Thus, for small values (less than 0.15), $F(X)$ was assumed to be constant and equal to $F(X=0.15)$; for high values of X (above 0.9), the function obtained between 0.15 and 0.9 was extrapolated. Although any value X_0 can be chosen as reference, it is important to choose a value obtained when the pore structure of the particles has opened, and experimental conditions have stabilized. In our case, we chose the value $X_0=0.5$, i.e. $F(0.5)=1$.

Theoretically, this determination should be done using intrinsic values of reactivity R , i.e. from experiments in which no limitation by heat or mass transfer occurs. Nevertheless, larger particles can also be used (Sorensen et al., 1996; Risnes et al., 2000). In order to check this, we first consider the surface function obtained with small particles (intrinsic values of R) and that obtained from the larger particles. We determined $F(X)$ as 5th-order polynomials. These two functions are plotted and compared in Fig. 8. As highlighted, the two curves are almost the same, allowing us to use the results obtained with the large particles to calculate the surface function.

The surface function was determined in H_2O , CO_2 , and O_2 atmospheres at 900 °C. The results are plotted in Fig. 9. Apart from a small irregularity in the case of CO_2 , all functions are monotonically increasing functions. These results show a weak influence of the partial pressure of the reacting gas on the appearance of the curves $F(X)$ in the different atmospheres. The discrepancy in the function in different partial pressure can be explained by the uncertainties in the experimental results. Consequently, the surface function for each atmosphere was

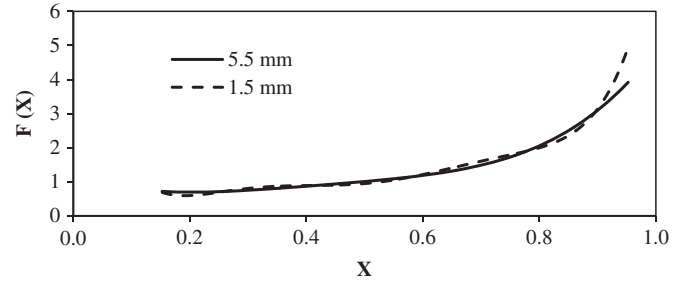


Fig. 8. Representation of surface function for the two cases of 1.5 and 5.5 mm particles. (temperature of bulk gas: 900 °C; 0.2 atm H_2O ; and particle size: 10.5 mm).

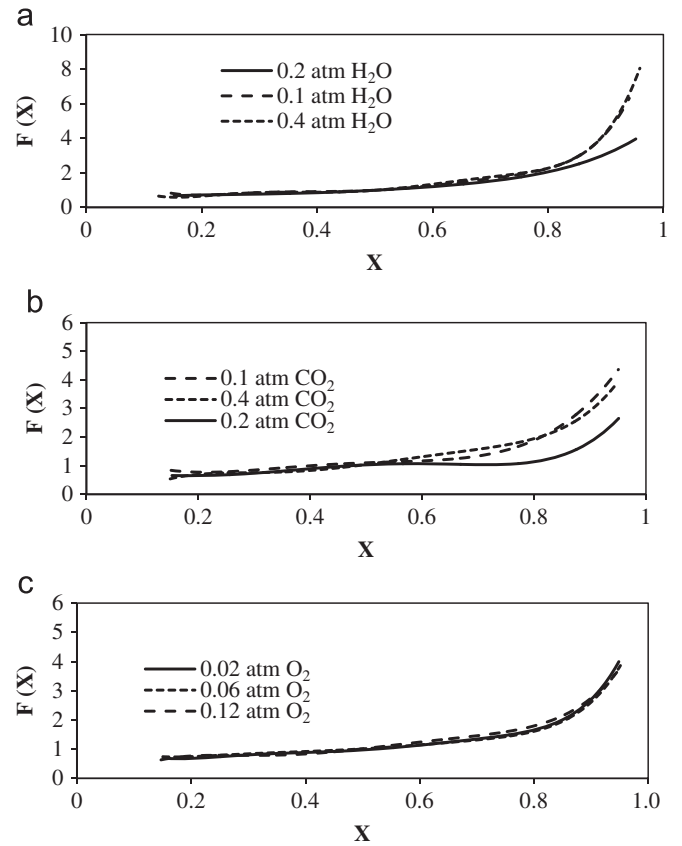


Fig. 9. The surface function for different atmospheres: H_2O (a), CO_2 (b), and O_2 (c). (temperature of bulk gas: 900 °C).

calculated as the average of the functions determined at each partial pressure.

The analytical expressions derived from experimental results are given by the following equations for H_2O :

CO_2 and O_2 atmosphere respectively

$$F(X) = 64.16X^5 - 129.72X^4 + 94.35X^3 - 29.39X^2 + 4.51X + 0.22 \quad (13)$$

$$F(X) = 90.90X^5 - 187.23X^4 + 135.12X^3 - 40.59X^2 + 5.55X + 0.65 \quad (14)$$

$$F(X) = 94.95X^5 - 190.37X^4 + 143.28X^3 - 47.08X^2 + 6.14X + 0.29 \quad (15)$$

3.2. Determination of kinetic parameters

The numerical model was compared with the experimental results (detailed in the previous section) obtained for a single

charcoal particle suspended in a macro-TG reactor and gasified successively in H₂O–N₂, CO₂–N₂, and O₂–N₂ atmospheres.

Given the uncertainty in the literature concerning the expression of the reaction rate, the first step consisted in fitting the reaction parameters to reproduce the experimental curves

Table 3
Intrinsic kinetic parameters.

H ₂ O	$k_{H_2O}^{int}$	A_1	35.5.10 ⁴	$s^{-1} atm^{-0.8}$
		E_{a1}	170.0	$kJ mol^{-1}$
		n	0.8	–
CO ₂	$k_{CO_2}^{int}$	A_2	120.10 ⁶	$s^{-1} atm^{-0.7}$
		E_{a2}	245.0	$kJ mol^{-1}$
		n	0.7	–
O ₂	$k_{O_2}^{int}$	A_3	1.10 ⁹	$s^{-1} atm^{-0.6}$
		E_{a3}	179.4	$kJ mol^{-1}$
		n	0.6	–

correctly. The values of kinetic parameters obtained are listed in Table 3. These kinetic constants are in good agreement with the synthesis proposed by Di Blasi (2009).

The results of the different simulations with varying char thickness, temperature, partial pressure, and nature of the reactant gas are compared with experimental results in Figs. 10–12.

It is of major importance to note here that the validity and uniqueness of kinetic constants is highly dependent on the correct description of external and internal heat and mass transfer in the model. Consequently the comparison of experimental and numerical results also aimed at finding the most suitable correction factor ξ (Eqs. (5) and (6)). We varied ξ between 0.1 and 10 and showed that a value of 1 was best to fit modeling results with experimental ones, in particular regarding the influence of particle thickness. Concerning the validation of internal transfers, we varied tortuosity since uncertainties exist in the literature regarding its value; we observed that a value of 5 was best to fit experimental and modeling results.

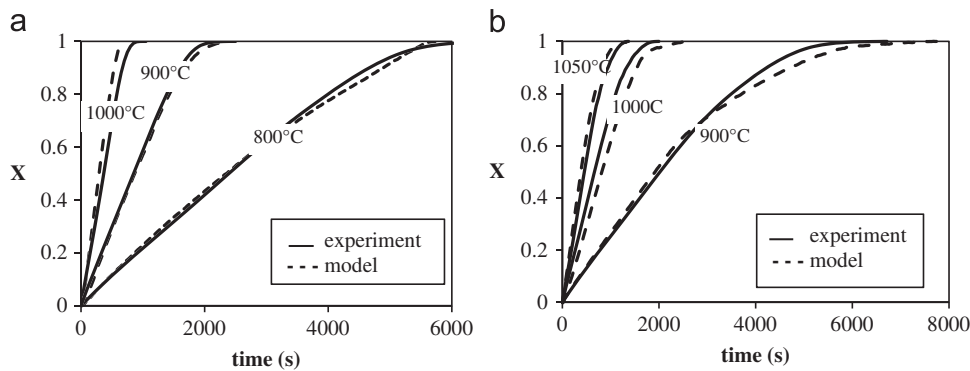


Fig. 10. Comparison of the model and experiments for three bulk gas temperatures in H₂O atmosphere (a) and CO₂ atmosphere (b) (partial pressure of reactant gas: 0.2 atm, particle thickness: 5.5 mm).

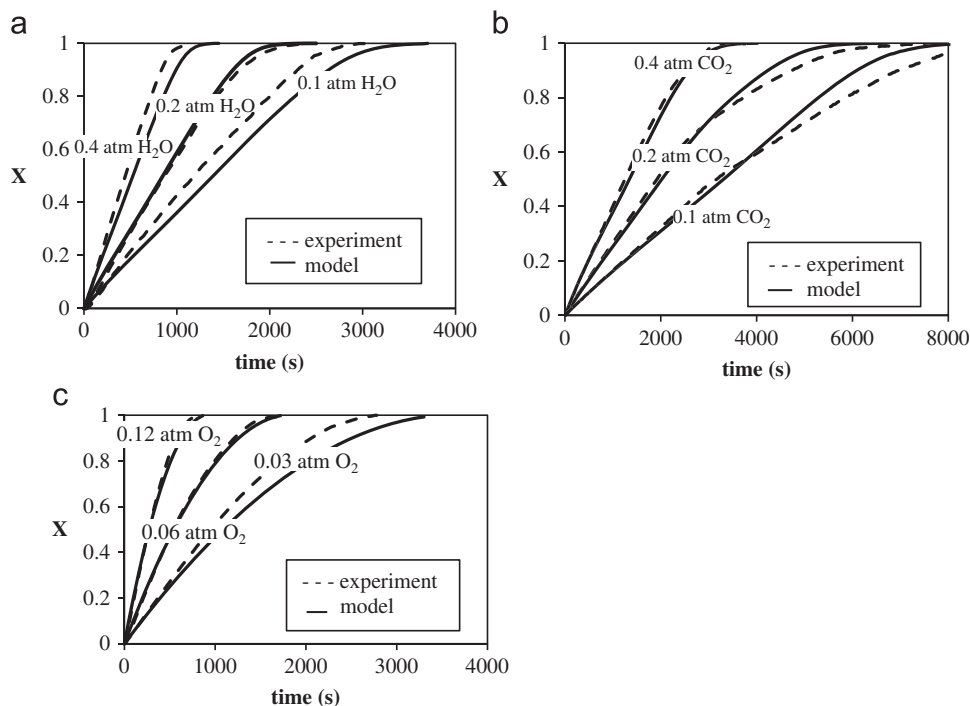


Fig. 11. Comparison of the model and experiments for three partial pressure of reactant gas: H₂O (a) and CO₂ (b) (temperature of bulk gas: 900 °C and particle thickness: 5.5 mm).

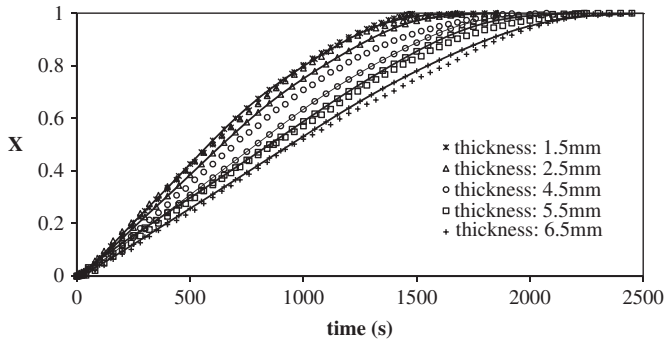


Fig. 12. Comparison of the experiments (symbol) and model (line+symbol) for different particle thicknesses (temperature of bulk gas: 900 °C, 0.2 atm H₂O, and particle size: 10.5 mm).

3.2.1. Influence of temperature

The gasification rate increases with an increase in temperature, as illustrated by simulations at different temperature both in H₂O/N₂ atmosphere (Fig. 10a) and CO₂/N₂ atmosphere (Fig. 10b). Simulations were performed for a 5.5-mm-thick particle placed in an atmosphere with H₂O partial pressure or CO₂ partial pressure of 0.2 atm. The sensitivity of the steam gasification or Boudouard reaction to the temperature was correctly recovered by the new model. This result supports the choice of kinetic and activation energy used for the model.

3.2.2. Influence of reactive gas partial pressure

Simulation results for charcoal reaction gasification in 0.1, 0.2, and 0.4 atm of H₂O (in N₂) and 0.1, 0.2 and 0.4 atm of CO₂ (in N₂) are illustrated respectively in Fig. 11a and b. Fig. 11c presents simulations of charcoal oxidation in 0.03, 0.06, and 0.12 atm of O₂ (in N₂). Operating conditions were 5.5-mm particle thickness and a temperature of 900 °C. The curves show good agreement between the model and experimental results even if slight discrepancies appear for steam gasification in 0.1 and 0.4 atm. However, the extent of this difference is not bigger than the experimental error. These figures support the choice of the kinetic schemes proposed in Eq. (8).

3.2.3. Influence of particle thickness

In order to check model sensitivity to particle thickness, we performed simulations in which we varied the particle thickness from 1.5 to 6.5 mm and compared with experimental results (Fig. 12). Here we focus the study on charcoal gasification in an atmosphere of 0.2 atm of H₂O (in N₂) and a temperature of 900 °C. It is notable that the model succeeds in reproducing the sensitivity of steam gasification to particle size. Indeed the simulation results show the same ratio of 1.6 as that measured experimentally between conversion times of smaller and bigger particles.

Differences between experiments and modeling, in particular for a 4.5 mm-thick particle, were attributed mainly to the heterogeneity between particles regarding morphology and composition.

3.3. Thermochemical behavior of the particle during gasification

From the previous section, we consider that our model correctly simulates the influence of both heat and mass transfer and the intrinsic kinetics on the global conversion progress, in the range of operating parameters considered (Table 2). In this section, we study the competition between the phenomenon involved in the gasification of a char particle. For this purpose the model can provide relevant information such as temperature profiles and the gas concentration inside the particle. In the

following, all the profiles inside the particle are plotted versus the half thickness, that is to say, considering a 5.5-mm thick particle, $x=0$ at the center of the particle and $x=2.75$ mm at the external surface.

We performed simulations in the following operating conditions: bulk gas temperature: 900 °C; particle thickness: 5.5 mm; 0.2 atm of H₂O or CO₂ and 0.06 atm of O₂.

First, steam gasification (Eq. (2)) was studied; partial pressure fields of H₂O, H₂, and CO are presented as a function of the thickness for a conversion of 0.25 (Fig. 13). This figure shows first that steam partial pressure at the particle surface, 0.185 atm, is close to the partial pressure in the bulk atmosphere, 0.2 atm, showing the limited influence of external mass transfers. Regarding internal mass transfers, H₂O partial pressure decreases from 0.185 atm at the surface to 0.13 atm at the center and shows steam diffusion limitation.

Fig. 14 compares reactive gas concentrations inside the particle for char-H₂O, char-CO₂ reactions, at two levels of conversion, 25% and 75%. Whatever the conversion progress, the decrease in CO₂ partial pressure during the Boudouard reaction is lower than the decrease in H₂O partial pressure during steam gasification. This result shows that mass transfer limitation inside the particle is higher for steam gasification than for the Boudouard reaction. This result is explained by the difference in the intrinsic reactivity of these two reactions, the slower the reaction, the smaller the internal mass transfer limitation. Regarding the changes in such profiles during conversion, the limitation decreases as the reaction progresses. At 75% of conversion, the decrease in the partial pressure of H₂O or CO₂ is negligible. This result is due to the increase in porosity with conversion that helps reactive gas diffusion. Moreover and only for these two reactions, the model

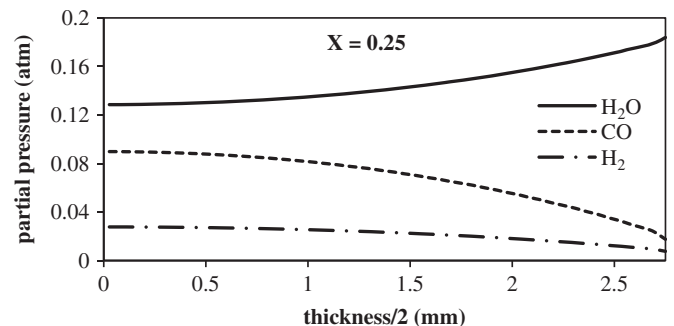


Fig. 13. H₂O, CO, and H₂ partial pressure profiles inside the particle at 0.25 conversion in the case of a gasification in 0.2 atm H₂O (temperature of bulk gas: 900 °C; particle thickness: 5.5 mm).

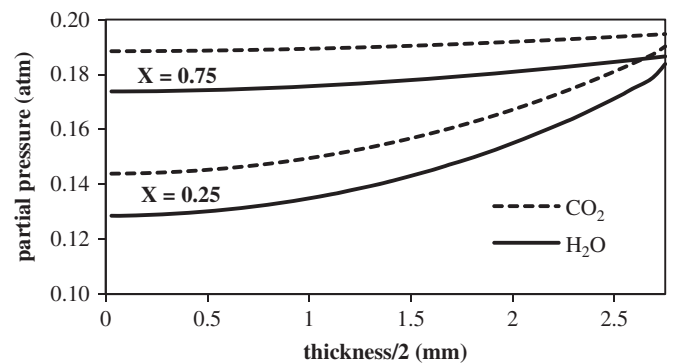


Fig. 14. H₂O (or CO₂) partial pressure profiles inside the particle at 0.25 and 0.75 conversion in the case of gasification in a 0.2 atm H₂O (or CO₂) (temperature of bulk gas: 900 °C; particle thickness: 5.5 mm).

shows that the thickness of the particle remains constant until about 95% of conversion, which is coherent with the increase in porosity.

The char-O₂ reaction leads to a very different behavior. Fig. 15 shows that the thickness of the char particle decreases during conversion and indicates a shrinking core of the particle during conversion in 0.06 atm O₂ atmosphere. Such behavior is due to mass transfer limitation. This result is confirmed in Fig. 16, where the profile of O₂ partial pressure is plotted for two conversion ratios. We can observe that the O₂ partial pressure falls abruptly from the partial pressure in the bulk atmosphere, i.e. 0.06 atm. The O₂ is rapidly and totally consumed in a zone close to the particle surface confirming an external or internal mass transfer limitation.

Finally, we focused on temperature profiles in char-H₂O, char-CO₂ and char-O₂ reactions. Regarding steam gasification and the Boudouard reaction, Fig. 17 shows that temperature at the surface of the particle is close to that of the bulk atmosphere: 891 and 896 °C for char-H₂O, char-CO₂ reactions, respectively. Inside the particle, the temperatures can be considered uniform, even if strictly speaking, there is a very slight decrease of 1–3 °C. Consequently, in the case of char-H₂O and of char-CO₂ these results show that no significant external and internal heat transfer limitation occurs. In practice, in these cases, models can be simplified assuming an isothermal particle.

Regarding the oxidation reaction, char-O₂, the model predicts an overheating of about 60 °C close to the particle surface (Fig. 17) due to exothermicity of the reaction. Inside the particle, the temperature remains constant, showing no internal heat transfer limitation.

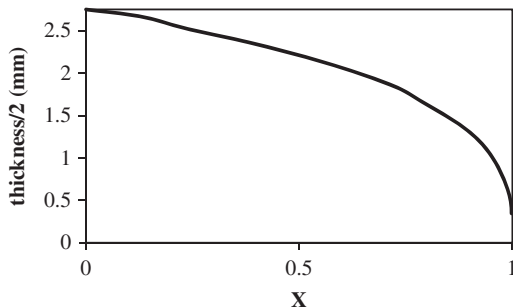


Fig. 15. Change in particle thickness during conversion in a 0.06 atm O₂ (temperature of bulk gas: 900 °C; particle thickness: 5.5 mm).

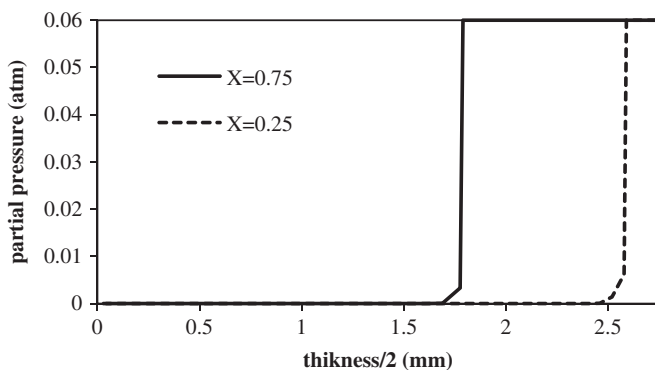


Fig. 16. O₂ partial pressure profiles inside the particle at 0.25 and 0.75 conversion in the cases of combustion in 0.06 atm O₂ (temperature of bulk gas: 900 °C; particle thickness: 5.5 mm).

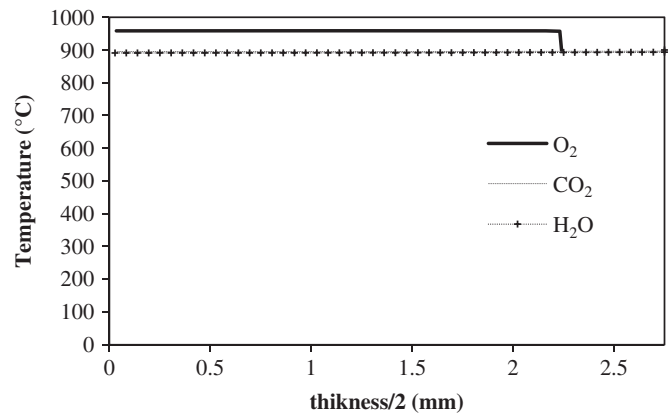


Fig. 17. Temperature profiles inside the particle at 0.5 conversion in the three atmospheres of 0.2 atm H₂O, 0.2 atm CO₂, and 0.06 atm O₂ (temperature of bulk gas: 900 °C; particle thickness: 5.5 mm).

These results demonstrate that the model succeeds in simulating the heterogeneous oxidation of char by a reactive gas whatever the limiting phenomena involved, i.e. kinetics or transfers. Hence, the model can predict a homogenous conversion inside the particle, a shrinking core conversion, or an intermediate situation between these two.

4. Conclusion

The gasification of wood char particles during gasification was thoroughly investigated in operating conditions relevant for industrial air gasifiers: temperature, 800–1000 °C; [H₂O]: 0.1–0.3 atm, [CO₂]: 0.1–0.3 atm, [O₂]: 0.03–0.12 atm.

This experimental study shows that, considering char from typical industrial wood chips, thickness was the critical dimension of the particle for the gasification process. The influence on the kinetics of the temperature, the nature and concentration of the gas were fully characterized for the three reactions: char-H₂O, char-CO₂, and char-O₂ thanks to an extensive parametric study. This exhaustive experimental data base will be very valuable for observation of parameter sensitivity and validation of particle models.

A previously developed numerical model was modified to take into account the non-spherical shape of particles, as well as changes in the morphological structure of the char by the introduction of a surface function $F(X)$. This function was determined experimentally and included in the model. The model can predict a homogenous conversion inside the particle, a shrinking core conversion, or an intermediate situation between the two. Comparison of the model with experimental data allowed the determination of the kinetic parameters needed to describe carbon conversion in three different atmospheres.

The model made it possible to characterize the thermochemical situation. We show that regarding gasification of char by H₂O or CO₂, the reaction is not limited by external or internal heat transfer phenomena, while there is a noticeable limitation by internal mass transfers. In O₂ atmosphere, the model predicts a shrinking core with overheating of the particle by 60 °C.

The experimental results, the kinetic parameter and surface function, and the characterization of the thermochemical situation, provide useful data to improve our understanding of the reactions involved in air gasifiers. Such results can be used into process models where equations are solved at the scale of the reactor, and in which the heat and mass source terms are required. These have to be calculated at the scale of the particle.

Nomenclature

X	conversion progress (dimensionless)
m	mass (kg)
ξ	correction factor (dimensionless)
k^{int}	intrinsic reactivity ($s^{-1} atm^{-n}$)
P	partial pressure (atm)
$F(X)$	surface function
R	Reactivity (s^{-1})
$C(t)$	concentration of active sites (dimensionless)

References

- Bhatia, S.K., Perlmutter, D.D., 1980. A random pore model for fluid-solid reactions: I. isothermal, kinetic control. *AIChE Journal*, 26, 379–386.
- Bhatia, S.K., Vartak, B.J., 1996. Reaction of microporous solids: the discrete random pore model. *Carbon* 34, 1383–1391.
- Biggs, M.J., Agarwal, P.K., 1997. The CO/CO₂ product ratio for a porous char particle within an incipiently fluidized bed: a numerical study. *Chemical Engineering Science* 52 (6), 941–952.
- Cetin, E., Gupta, R., Moghtaderi, B., 2005. Effect of pyrolysis pressure and heating rate on radiata pine char structure and apparent gasification reactivity. *Fuel* 84, 1328–1334.
- Cho, Y.S., Joseph, B., 1981. Heterogeneous model for moving-bed coal gasification reactors. *Industrial & Engineering Chemical Process Design and Development* 20, 314.
- Dasappa, S., Paul, P.J., Mukunda, H.S., Shrinivasa, U., 1994. The gasification of wood-char sphere in CO₂-N₂ mixtures: analysis and experiments. *Chemical Engineering Science* 49, 223–232.
- De Diego, L.F., Garcia-Labiano, F., Abad, A., Gayan, P., Adanez, J., 2002. Modeling of the devolatilization of nonspherical wet pine wood particles in fluidized beds. *Industrial & Engineering Chemistry Research* 41, 3642–3650.
- Di Blasi, C., 2000. Dynamic behaviour of stratified downdraft gasifiers. *Chemical Engineering Science* 55, 2931–2944.
- Di Blasi, C., 2009. Combustion and gasification rates of lignocellulosic chars. *Progress in Energy and Combustion Science* 35, 121–140.
- Dutta, S., Wen, C.Y., Belt, R.J., 1977. Reactivity of coal and char. 1. In carbon dioxide atmosphere. *Industrial and Engineering Chemistry Process Design and Development* 16, 20–30.
- Dutta, S.C., Wen, Y., 1977. Reactivity of coal and char. 2. In oxygen-nitrogen atmosphere. *Industrial and Engineering Chemistry Process Design and Development* 16, 31–36.
- Fassinou, W.F., Van de Steene, L., Toure, S., Volle, G., Girard, P., 2009. Pyrolysis of Pinus pinaster in a two-stage gasifier: influence of processing parameters and thermal cracking of tar. *Fuel Processing Technology* 90, 75–90.
- Groeneveld, M.J., van Swaaij, W.P.M., 1980. Gasification of char particles with CO₂ and H₂O. *Chemical Engineering Science* 35, 307–313.
- Harris, D.J., Smith, I.W., 1990. Intrinsic reactivity of petroleum coke and brown coal char to carbon dioxide, steam and oxygen. *Proceedings of the Combustion Institute* 23, 1185–1190.
- Henriksen, U., Hindsgaul, C., Qvale, B., Fjellerup, J., Jensen, A.D., 2006. Investigation of the anisotropic behavior of wood char particles during gasification. *Energy Fuels* 20, 2233–2238.
- Hobbs, M.L., Radulovic, P.T., Smoot, L.D., 1993. Combustion and gasification of coal in fixed-beds. *Progress in Energy and Combustion Science* 19, 505.
- Klose, W., Wolki, M., 2005. On the intrinsic reaction rate of biomass char gasification with carbon dioxide and steam. *Fuel* 84, 885–892.
- Knoef, H.A.M. (Ed.), Biomass Technology Group.
- Kovacik, G., Chambers, A., Ozum, B., 1991. CO₂ gasification kinetics of two Alberta coal chars. *The Canadian Journal of Chemical Engineering* 69, 811–815.
- Kumar, M., Gupta, R.C., 1994. Influence of carbonization conditions on the gasification of Acacia and Eucalyptus wood chars by carbon dioxide. *Fuel* 73, 1922–1925.
- Mermoud, F., Salvador, S., Van de Steene, L., Golfier, F., 2006. Influence of the pyrolysis heating rate on the steam gasification rate of large wood char particles. *Fuel* 85, 1473–1482.
- Mermoud, F., Golfier, F., Salvador, S., Van de Steene, L., Dirion, J.L., 2006. Experimental and numerical study of steam gasification of a single charcoal particle. *Combustion & Flame* 145 (1-2), 59–79.
- Moilanen, A., Saviharju, K., Harju, T., 1993. Steam gasification reactivities of various fuel chars. In: Bridgwater, A.V. (Ed.), *Advances in Thermochemical Biomass Conversion*. Blackie Academic & Professional, pp. 131–141.
- Rensfelt, E., Blomkvist, G., Ekstrom, C., Engstrom, S., Espents, B.G., Linnanki, L., 1978. Basic gasification studies for development of biomass medium-btu gasification processes. In: *Proceedings of Energy for Biomass and Waste, IGT Symposium*, Washington D.C., August 14–18, 1978, pp. 466–494.
- Risnes, H., Sorensen, L.H., Hustad, J.E., 2000. Reactivity of chars from wheat, spruce and coal. In: Bridgwater, A.V. (Ed.), *Progress in Thermochemical Biomass Conversion*. Tyrol.
- Roberts, D.G., Harris, D.J., 2000. Char gasification with O₂, CO₂ and H₂O: effects of pressure on intrinsic reaction kinetics. *Energy and Fuels* 14, 483–489.
- Sharma, A.K., Kyotani, H., Tomita, A., 2002. Effect of microstructural changes on gasification reactivity of coal chars during low temperature gasification. *Energy & Fuels* 16, 54–61.
- Sorensen, L.H., Gjernes, E., Jessen, T., Fjellerup, J., 1996. Determination of reactivity parameters of model carbons, cokes and flame-chars. *Fuel* 75, 31–38.
- Standish, N., Tanjung, A.F.A., 1988. Gasification of single wood charcoal particles in CO₂. *Fuel* 67, 666–672.
- Tagutchou, J.P., 2008. *Gazéification de Charbon de Plaquettes Forestières: Particule Isolée et Lit Fixe Continu*. Thèse de Doctorat, Cirad, ED 305, Université de Perpignan.
- Van den Aarsen, F.G., Beenackers, A.A.C.M., Van Swaaij, W.P.M., 1985. Wood pyrolysis and carbon dioxide char gasification kinetics in a fluidized bed. In: Overend, R.P., Milne, T.A., Mudge, L.K. (Eds.), *Fundamentals of Thermochemical Biomass Conversion*. Elsevier, New York, pp. 691–715.
- Ye, D.P., Agnew, J.B., Zhang, D.K., 1998. Gasification of a south Australian low-rank coal with carbon dioxide and steam: kinetics and reactivity studies. *Fuel* 77, 1209–1219.